Macromolecules

ARTICLE

pubs.acs.org/Macromolecules

Tuning Polymer Blends to Cocontinuous Morphology by Asymmetric Diblock Copolymers as the Surfactants

Gongwei Pu, Yingwu Luo,* Anni Wang, and Bogeng Li

The State Key Laboratory of Chemical Engineering, Department of Chemical and Biological Engineering, Zhejiang University, Hangzhou 310027, P. R. China

ABSTRACT:

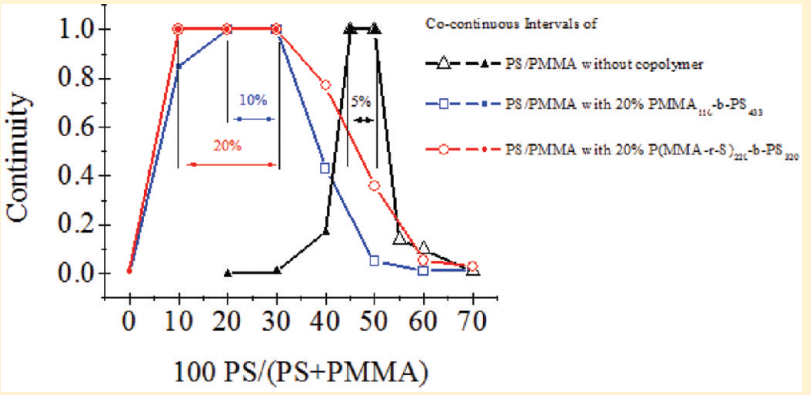

We investigated the influence of the chain asymmetry of the styrene (S)−methyl methacrylate (MMA) copolymer (surfactant) on the morphology of the polystyrene (PS)/poly(methyl methacrylate) (PMMA) blends. It was, for the first time, demonstrated that the chain asymmetry of the block copolymer surfactant would have significant influence on the structure of the polymer blend in the melt mixing process. In the PS/PMMA = 30/70 blends, the addition of asymmetric AB diblock copolymers tuned the morphology from the droplet-in-matrix structure to the cocontinuous structure. At 20 wt % asymmetric AB block copolymer ($PMMA_{110}$-*block*-PS_{430}) dosage, the onset of the cocontinuous interval of the PS/PMMA blends was lowered to PS/PMMA = 20/80 and the cocontinuous interval was broadened to PS/PMMA = 20/80−30/70, compared with the onset at PS/PMMA = 45/55 and the interval at PS/PMMA = 45/55−50/50 of the PS/PMMA blends without the copolymers. The reason was that the packing of the asymmetric block copolymer on the interface provided the bending energy being against the interfacial energy when the longer block of the copolymer was in the minor phase side, suppressing the breakup of the minor phase fibers during melt mixing. With the addition of 20 wt % AC block copolymer ($P(S\text{-}ran\text{-}MMA)_{220}$-*block*-$PS_{320}$), which was more asymmetric than the AB block copolymer ($PMMA_{110}$-*block*-PS_{430}) of the same molecular weight and monomer composition, the PS/PMMA blends showed an even wider cocontinuous interval at PS/PMMA = 10/90−30/70.

1. INTRODUCTION

The morphology of a polymer blend is critical for the performance. Droplet-in-matrix morphology is the most common type compared with fiber, lamellar, and other morphologies. Recently, the polymeric composites with the cocontinuous structure on submicrometer scale are attracting wider and wider interest for the great enhancement of mechanical,[1] optical,[2] conductive,[3] and transporting properties.[4] Also, cocontinuous structured composites can be used as templates to prepare the materials for controlled drug release[5] and to prepare nanosheath materials.[6]

The cocontinuous structured polymeric composites can be prepared by both thermodynamic and kinetic methods. The thermodynamically stable cocontinuous structure had been theoretically predicted and experimentally verified by Bates et al.[7,8] They reported that in a polyethylene (PE)/polyethylenepropylene (PEP) = 1:1 system at 119 °C the cocontinuous structure could be achieved in a narrow window when 0.09%−0.12% PE−PEP diblock was added into the system. Unfortunately, tens of hours were needed to achieve the equilibrium state.[9] The cocontinuous morphology can also be obtained by simply mechanically mixing the melts of two immiscible polymers. In this case, Favis et al.[10,11] summarized that the cocontinuous morphology should be the result of the coalescence of the minor phase domains in the forms of droplets or threads. The composition of the two polymers to form the cocontinuous morphology is mainly determined by the viscosity ratio and interfacial tension.[12,13] The formed cocontinuous structure is not thermodynamically stable but can be frozen quickly after melt processing.

Received: November 23, 2010
Revised: January 14, 2011
Published: March 16, 2011

Table 1. Structure Information of Homo- and Copolymers

polymer	M_n (g/mol)	M_w (g/mol)	monomer composition (f_{St})	viscosity at 100 s^{-1} at 200 °C (Pa s)
PS	121 000	238 400		1484
PMMA	49 800	83 700		2469
AB1 ($PMMA_{110}$-*b*-PS_{110})	22 000	25 700	0.54	
AB2 ($PMMA_{110}$-*b*-PS_{211})	32 100	44 900	0.71	
AB3 ($PMMA_{110}$-*b*-PS_{433})	54 300	65 200	0.81	
AC[a] (PS_{320}-*b*-P(St-*r*-MMA)$_{220}$)	54 000	76 700	0.82	

[a] $f_{St} = f_{MMA} = 0.5$ in the random block of AC. The footnote means the degree of polymerization.

The thermodynamics of the microphase separation of the diblock copolymer has been widely investigated.[14−17] The asymmetry of the diblock copolymer, i.e., the ratio of the molecular weight of the two blocks, actually the volume ratio of the two blocks on different sides of the interface, plays a very important role to determine the morphology of the microphase separation. Matsen et al.[15] reported that phase transitions from lamellae to cylinders to spheres occurred due to the increasing spontaneous curvature as the asymmetry of the diblock copolymer increased. Such spontaneous curvature, also understood as bending energy,[18−20] can be used to tune the morphology of the thermodynamically stable microemulsion systems. Balsara et al.[21,22] managed to tune the morphology of 50/50 PE/polyisobutylene (PIB) mixture from lamellar phases to single droplet microemulsions to bicontinuous microemulsions by altering the PE−PP block copolymer geometry on the interface through the temperature. The so-called "balanced surfactant" is actually the balance of the bending energy of the surfactant layer and the interfacial energy of the PE/PIB mixture. Such findings are in consistence with the case in the small molecular oil−water−surfactant emulsion systems. It is well accepted that the symmetry of the surfactants is decisive for the emulsion forms, especially in the surfactant concentrated emulsion systems.[23]

The kinetic melt mixing of the binary immiscible polymer blends usually needs polymeric surfactants, the copolymers, for compatibilization. The copolymers acting as surfactants can locate at the interface between the two phases, lower the interfacial tension, promote the interfacial adhesion, and prevent the minor phase domains from coalescence to get a reduced characteristic size of the minor phase.[24−29] The molecular structure of the polymeric surfactant was found to have significant influence on the efficiency to reduce the characteristic size. It was reported that the symmetric diblock copolymer was the most effective structure to reduce the interfacial tension if the molecular weight was fixed.[30−32] Although the higher molecular weight of the copolymer gives the higher interfacial activity, an optimal molecular weight is always existed to reach the best emulsification effect for the balance of the interfacial activity and the migration ability.[28,33] Leal et al. proved that, compared with the effect of reducing the interfacial tension to enhance the breakup of the minor phase domains, the major effect of the copolymers on the interface is to inhibit the coalescence of the minor phase domains.[34−36] Because of the suppressed coalescence between the minor phase domains, the addition of the polymeric surfactants usually narrows the cocontinuous interval of the blends. Willis et al. observed a narrowed composition interval of the cocontinuous structures when adding polyethylene-based ionomer into the polypropylene/polyamide blends.[37] Zhang et al. reported that the addition of PS-*graft*-PA6 narrowed the cocontinuous interval of the PS/PA6 blends, from 40/60−65/35 (without PS-*graft*-PA6) to 45/55−65/35 (with PS-*graft*-PA6).[38]

To our best knowledge, the influence of the asymmetry of the polymeric surfactant on the structure of the binary immiscible polymer blends during melt mixing was not investigated yet. In this article, we used polystyrene (PS)/poly(methyl methacrylate) (PMMA) as a model blending system to investigate this topic. We would demonstrate the chain asymmetry of the polymeric surfactant could exert a significant influence on the structure of the blend. Most interestingly, the asymmetric block copolymer could broaden and shift the cocontinuous interval of the PS/PMMA blends.

2. EXPERIMENTAL DETAILS

Materials. PS and PMMA were purchased from BASF-YPC. The copolymers used as the polymeric surfactants were synthesized via RAFT polymerization, as described in our previous works.[39−41] The molecular weight and its distribution were determined by GPC, while the monomer composition of the copolymer was determined by ^{1}H NMR.[39−41] The structure information on these (co)polymers is summarized in Table 1.

Blend Preparation. All the blends were prepared by mixing the components in a Brabender twin rotor mixer (W50EHT, Brabender Measurement & Control System). All components were added in the form of pellets or powders simultaneously and mixed under the rotor speed of 100 rpm (shear rate ≈ 100 s^{-1}) at 200 °C for 15 min. Judging from the GPC curves of the samples before and after mixing, no chain degradation was observed during the compounding. The melt blends were then removed quickly from the mixer and cooled in air to freeze the morphology. Part of the products was then annealed in the quiescent condition under vacuum at 200 °C to investigate the annealed morphology.

Morphology Analysis. Samples were cut to ultrathin films with thickness of 50−100 nm at room temperature with Power Tome PC ultramicrotome (RMC Co.). The morphology was observed under a JEM-1230 transmission electron microscope (TEM) operated at 80 kV. In all images, the white area was the PMMA phase and the dark area was the PS phase.

An in-house software was applied to analyze the TEM images to derive the characteristic size of the morphology. If the morphology was droplet-in-matrix, the areas (A_i) of more than 200 domains were derived by the software and then the number-averaged diameter ($D_n = (\Sigma_{i=1}^{N} D_i)/N$, where $D_i = (4A_i/\pi)^{1/2}$ and N is the number of the calculated particles) and volume-averaged diameter ($D_v = \Sigma D_i^3/\Sigma D_i^2$) were calculated. Otherwise, the characteristic size (D) of the morphology was first manually labeled at more than 200 locates and then counted by the software.

Solvent Extraction. The solvent extraction method was used to quantify the continuity of each phase in the blends. Samples were cut to

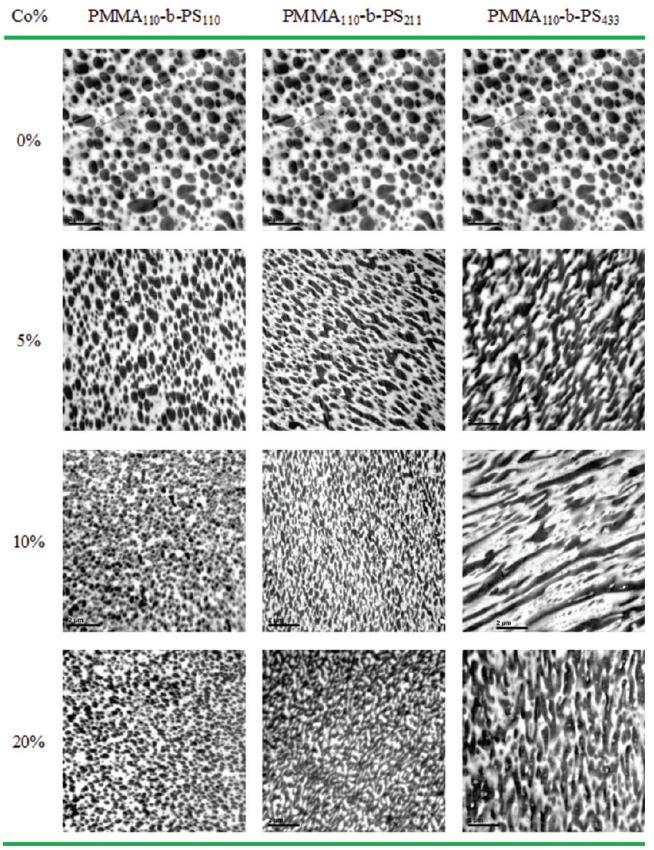

Figure 1. TEM images of the blends of PS/PMMA/PMMA-*b*-PS = $0.3(100 - k)/0.7(100 - k)/k$ (wt %), where k is the dosage of the AB block copolymers and $k = 0, 5, 10, 20$ as listed in the first column. All the images are 11.5 μm × 11.5 μm.

the same thickness and weight to make sure that the results were comparable.[42] PS and the copolymers were extracted by cyclohexane at 40 °C for over 10 days until a constant weight of the remainder achieved. PMMA was extracted by formic acid at 60 °C in the same way. The gravimetric method was used to calculate the extent of the continuity according to eqs 1 and 2.

$$\%\text{PS continuity} = \frac{(\text{wt of PS and PS-}co\text{-PMMA})_{\text{initial}} - (\text{wt of PS and PS-}co\text{-PMMA})_{\text{final}}}{(\text{wt of PS and PS-}co\text{-PMMA})_{\text{initial}}} \times 100\% \quad (1)$$

$$\%\text{PMMA continuity} = \frac{(\text{wt of PMMA})_{\text{initial}} - (\text{wt of PMMA})_{\text{final}}}{(\text{wt of PMMA})_{\text{initial}}} \times 100\% \quad (2)$$

BET Measurement. The AUTOSORB-1-C (Quantachrome Co.) was used to measure the specific interfacial area of the cocontinuous specimens. The cyclohexane-extracted porous samples with PS phase removed were cut into small pieces for the BET test. The multiple point BET method was used to treat the result and to derive the specific interfacial area, as introduced in Favis et al.'s work.[43] Because the glass transition temperatures of the samples were 105−110 °C, the degassing process was operated at 90 °C under vacuum over one night.

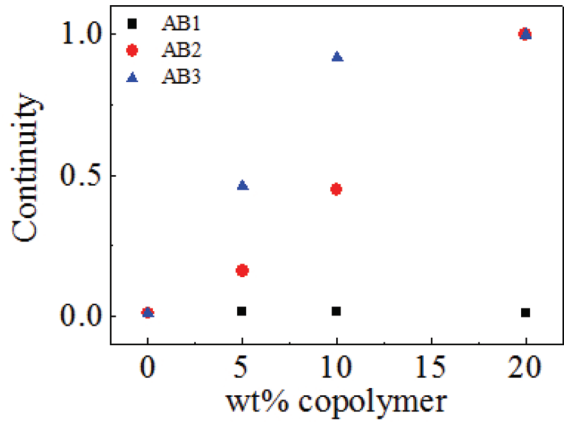

Figure 2. Continuities of the PS phase in the blends of PS/PMMA/PMMA-*b*-PS = $0.3(100 - k)/0.7(100 - k)/k$ (wt %), where k is the dosage of the block copolymers and $k = 0, 5, 10, 20$. (square) AB1 = $PMMA_{110}$-*b*-PS_{110}, (circle) AB2 = $PMMA_{110}$-*b*-PS_{211}, (triangle) AB3 = $PMMA_{110}$-*b*-PS_{433}.

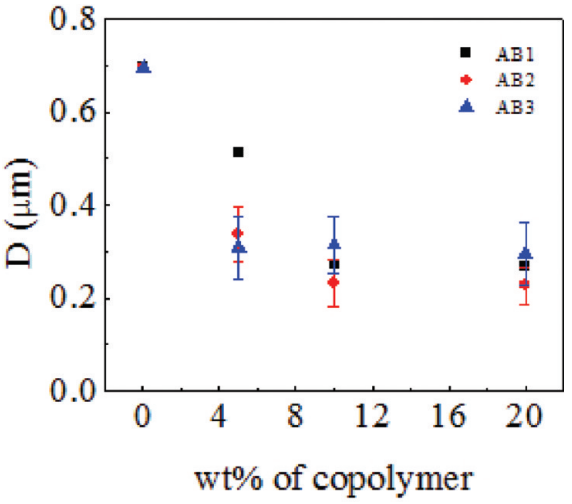

Figure 3. Characteristic size of the PS phase in the blends of PS/PMMA/PMMA-*b*-PS = $0.3(100 - k)/0.7(100 - k)/k$ (wt %), where k is the dosage of the copolymers and $k = 0, 5, 10, 20$. (square) AB1 = $PMMA_{110}$-*b*-PS_{110}, (circle) AB2 = $PMMA_{110}$-*b*-PS_{211}, (triangle) AB3 = $PMMA_{110}$-*b*-PS_{433}.

Table 2. Specific Interfacial Area and the Interfacial Coverage of the Copolymers in PS/PMMA/AB2 = 24/56/20 and PS/PMMA/AB3 = 24/56/20

blend composition	specific interfacial area (S) (m^2/g)	interfacial coverage (Σ) (chain/nm^2)
PS/PMMA/AB2 = 24/56/20	9.267	0.405
PS/PMMA/AB3 = 24/56/20	5.636	0.393

3. RESULTS AND DISCUSSION

Influence of the Asymmetry of the Polymeric Surfactant on the Morphology of the PS/PMMA = 30/70 Blends. We set the ratio of the homopolymers as PS/PMMA = 30/70. Under such a composition, the PS-droplet-in-PMMA-matrix morphology was observed when no polymeric surfactant was added.

dx.doi.org/10.1021/ma1026719 |*Macromolecules* 2011, 44, 2934–2943

Scheme 1. Aggregation of the PS Blocks on the PS Fiber Inner Side of the PS/PMMA Interface Suppresses the Breakup of the PS Fibers during Melt Mixing

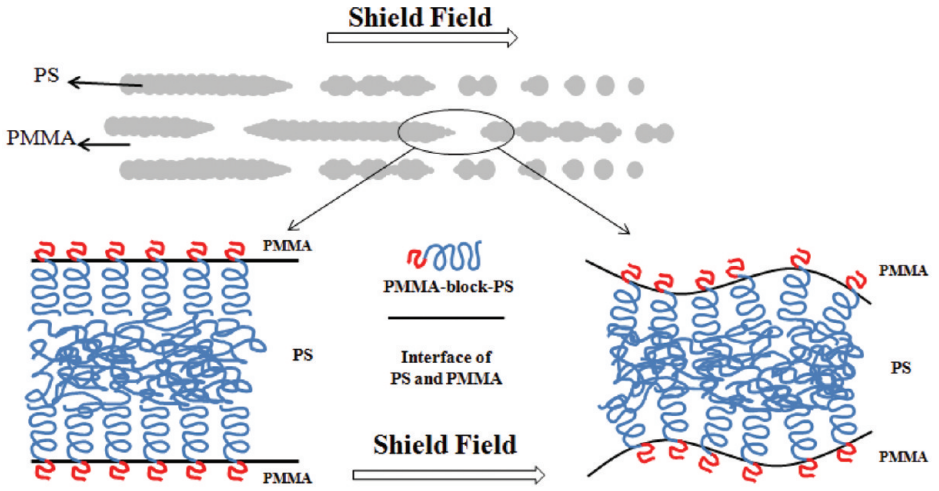

To investigate the effect of the asymmetry of the polymeric surfactant on the blend structure, a series of the AB block copolymers, PMMA-*b*-PS, with different asymmetries were synthesized. The degrees of polymerization (DP) of the PMMA blocks were the same for all AB block copolymers, but the DPs of the PS blocks were altered. Such design made sure that the asymmetry was tuned by the varied length of PS block, and the steric protection effect of the minor phase domains from coalescence remained similar, which was highly dependent on the PMMA block length in the continuous PMMA phase based on the Lyu et al.'s reports.[25,44,45]

The series of PMMA-*b*-PS with different asymmetries was respectively added to the blend system. The resulted morphologies of the blends are shown in Figure 1. As the symmetric AB block copolymer, $PMMA_{110}$-*b*-PS_{110} (AB1), added into the blend, the structure of the blends remained droplet-in-matrix for all copolymer dosages even up to 20%. Such observations were in agreement with the literature.[25,28,44,46] As the asymmetric block copolymers, $PMMA_{110}$-*block*-PS_{211} (AB2) and $PMMA_{110}$-*block*-PS_{433} (AB3), added into the blends, the dispersed PS phase was gradually stretched to form long twisted fibers with the increase of the copolymer dosages and the PS fibers connected each other to form cocontinuous structure at 20% copolymer dosage. It is interesting that when the AB block copolymer became asymmetric, the structure of the blend changed from droplet-in-matrix into cocontinuous.

Figure 2 shows the PS phase continuity curves of the blends corresponding to Figure 1. The continuity was estimated by the solvent extraction method. As seen in the continuity diagram, the addition of the symmetric AB1 block copolymer into the PS/PMMA = 30/70 blends did not increase the continuity of the dispersed PS phase at all. The continuities of the PS phase in the blends with AB3 were much higher than those in the blends with AB2 when the dosages of the AB block copolymers were 5% and 10%. Both the asymmetric block copolymers (AB2 and AB3) increased the continuity of the PS phase up to the unit at 20% dosage. It is clear that the higher asymmetry of the polymeric surfactant leads to the higher tendency to form the cocontinuous structure.

The statistical results of the characteristic size of the PS phase in the PS/PMMA/PMMA-*b*-PS blends are shown in Figure 3. In this emulsification diagram, the characteristic size of the PS phase

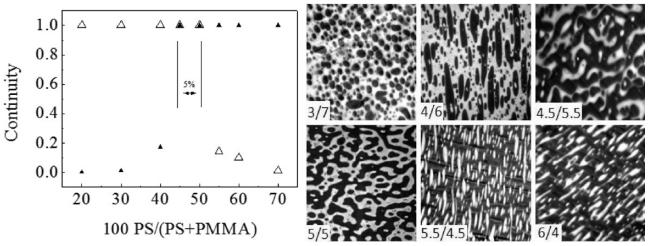

Figure 4. Cocontinuous interval of the PS/PMMA blends without copolymers and the corresponding TEM images. All the images are 11.5 μm × 11.5 μm, and the ratios of PS/PMMA are listed at lower left corner. The continuity of the PS phase (filled triangle) was detected by cyclohexane extraction and the continuity of the PMMA phase (hollow triangle) was detected by formic acid extraction.

decreased with the increase of the copolymer dosages and leveled off after 10%, 10%, and 5% copolymer dosages for AB1, AB2, and AB3, respectively. For AB1, the leveling off of the characteristic size meant that no more interfacial area was created. However, for AB2 and AB3, the total area of the interface was still increasing with the increase of the copolymer dosages in the leveling off region, since the continuity of the PS phase was still increasing, as seen in Figure 2. Also as evidenced in Figure 3, the AB2 block copolymer had the best emulsification ability for the PS/PMMA blends among the three kinds of AB block copolymers when the copolymer dosages exceeded 10%, which was probably due to a good balance between the interfacial activity and transportation rate of the copolymers.[28,47−50]

Table 2 gives the specific interfacial areas (S) for two cocontinuous structured blends, PS/PMMA/AB2 = 24/56/20 and PS/PMMA/AB3 = 24/56/20. Given the specific interfacial areas of the samples, the interfacial coverage of the block copolymer (Σ) was calculated by eq 3 by assuming that all the copolymers should stay on the interface.

$$\Sigma = \frac{\text{number of the copolymer chain per weight of the blend}}{\text{specific interfacial area of the blend}} \quad (3)$$

dx.doi.org/10.1021/ma1026719 |*Macromolecules* 2011, 44, 2934–2943

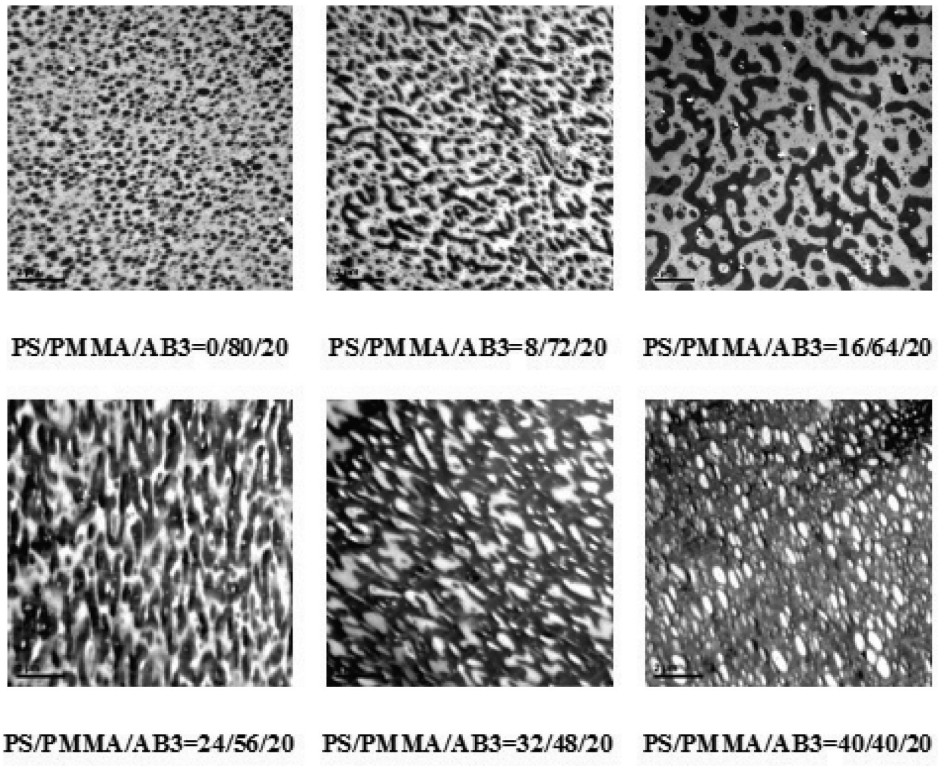

Figure 5. TEM images of PS/PMMA blends of various homopolymer ratios with 20% asymmetric AB3 block copolymer, $PMMA_{110}$-*b*-PS_{433}. The compositions of the blends are listed under each image. All the images are 11.5 μm × 11.5 μm.

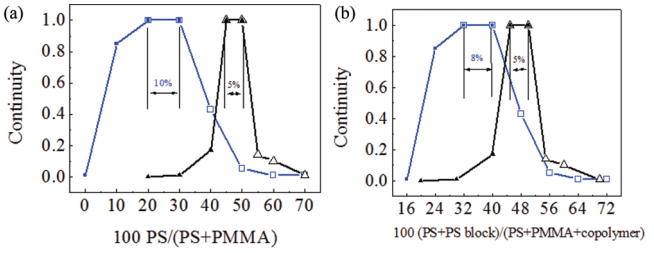

Figure 6. Cocontinuous interval of PS/PMMA blends (blue line + square) with 20% asymmetric copolymer, $PMMA_{110}$-*b*-PS_{430} (AB3) compared with that (black line + triangle) without the copolymer. Continuity of PS (filled scatters) was detected by cyclohexane extraction and continuity of PMMA (hollow scatters) was detected by formic acid extraction. The width of the composition intervals of cocontinuous structures are marked on the figure. The compositions of the blends should be expressed as (a) PS/PMMA/AB3 = $0.8x/0.8(100 - x)/20$, where x is the PS homopolymer fraction in homopolymers. (b) PS/PMMA/AB3 = $(x - 16)/(96 - x)/20$, where x is the total PS fraction in the blends contributed by both PS homopolymer and PS block of AB3.

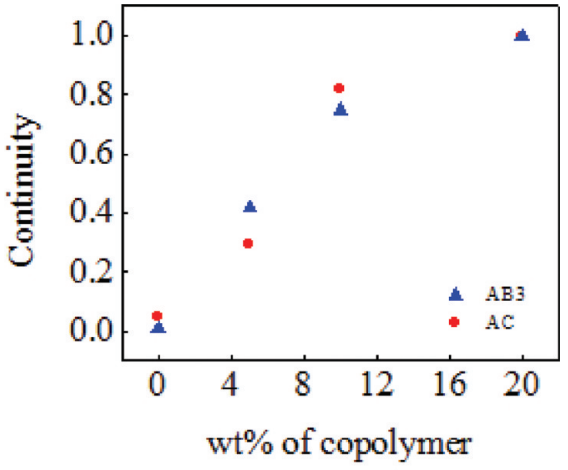

Figure 7. Continuity of the PS phase in the blends of PS/PMMA/copolymer = $0.3(100 - k)/0.7(100 - k)/k$ (wt %), where k is the dosage of the copolymer and k = 0, 5, 10, 20. (circle) AC = P(MMA-*ran*-S)$_{220}$-*b*-PS_{320}, (triangle) AB3 = $PMMA_{110}$-*b*-PS_{433}.

As listed in Table 2, the estimated interfacial coverage was very high. It is worthy pointing out that the estimated interfacial coverage might be overestimated considering that some of the added block copolymer might not stay at the interface and some pores of the samples might collapse during solvent extraction. Unfortunately, it is extremely difficult to obtain the amount of the block copolymer on the interface. Usually, one can indirectly judge the formation of the copolymer micelles from the emulsification curves. In the cocontinuous cases, the formation of the micelles can be derived from the level-off in the plots of the characteristic size and the continuity versus copolymer dosage. Considering the changing trends shown in Figures 2 and 3, we believe that most of the block copolymer might be located on the interface.

According to Favis et al.'s theory,[10] the formation of the cocontinuous structure in a binary immiscible blend is due to the coalescence of the minor phase domains, which has been supported by many reports.[37,38,51−54] The addition of the polymeric surfactants commonly narrows the cocontinuous interval of the

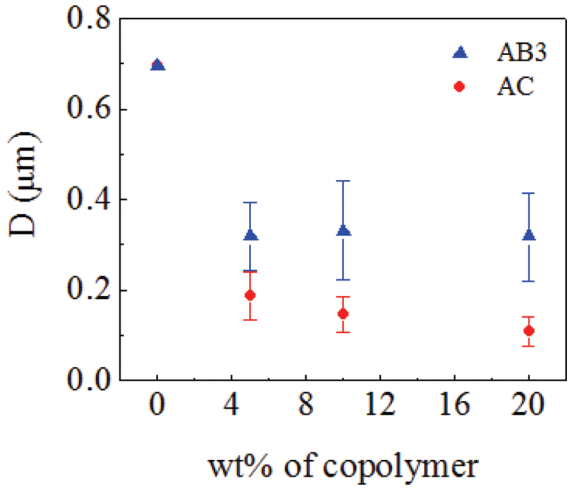

Figure 8. Characteristic size of the PS phase in the blends of PS/PMMA/copolymer = $0.3(100 - k)/0.7(100 - k)/k$ (wt %), where k is the dosage of the copolymers and $k = 0$, 5, 10, 20. (circle) AC = P(MMA-*ran*-S)$_{220}$-*b*-PS$_{320}$, (triangle) AB3 = PMMA$_{110}$-*b*-PS$_{433}$.

binary immiscible polymer blends, since the coalescence is suppressed. Compared with the reduction of the interfacial tension and other factors, the steric repulsion effect of the polymeric surfactant is dominant in controlling the coalescence of the minor phase domains.[25,34−36,44,45] In the current cases, the PMMA blocks of the AB block copolymers, which protected the minor PS phase from the coalescence, had the same DPs. So, the steric repulsion effect should be similar for all the block copolymers used in the current cases. It is suggested that the formation of the cocontinuous structure in our current cases was facilitated by the asymmetry of the block copolymer rather than the coalescence.

In the shear field during the melt mixing, the dispersed domains usually undergo the three-stage deformation. The dispersed domains are first stretched to form fibers. The stretched fibers become instable because of the capillary force. The breakup of the fibers is controlled by the capillary number, *Ca*, defined as $\eta_m R\dot{\gamma}/\sigma$, where η_m, R, $\dot{\gamma}$, and σ are the viscosity of matrix, the diameter of the fiber, the shear rate, and the interfacial tension, respectively. The breakup takes place when *Ca* is larger than the critical capillary number Ca_c.[34,35,46,55] Finally, the nonregular-shaped fragments retract to form droplets to minimize the total interfacial area. According to the literature,[56,57] the capillary breakup process can be described in detail as shown in Scheme 1. When a polymeric fiber is embedded in another immiscible polymeric matrix, the distortions first appear at the surface of the fiber. These distortions grow in the direction of the shearing field, leading to the breakup of the fibers.[56,57]

In our cases, the AB2 and AB3 block copolymers were asymmetric with the longer block extended into the minor phase. The packing of these asymmetric block copolymer molecules on the interface provided extra energy of conformational repulsion, also called as bending stress.[18−20] For the convenience in discussion, we set the curvature caused by interfacial tension as positive, i.e., favoring the PS-droplet-in-PMMA-matrix structure. Thus, the bending stress should have the opposite effect to the interfacial tension, favoring the negative curvature of the interface. When the packing density of the block copolymers on the interface was large enough, i.e., the bending energy could balance the interfacial energy, the breakup process of the minor phase fibers should be suppressed. As a result of the packing or folding of the minor phase fibers, the fully cocontinuous morphology was achieved. Accordingly, the AB block copolymer with the larger asymmetry led to more negative curvature at the same packing density so that the continuity of the minor phase in the corresponding blend increased faster, as seen in Figure 2. Fortelny et al. observed that the PS/PE = 80/20 blend had the cocontinuous structure when compatibilized by PS$_{100}$-*block*-PB$_{1111}$ (PB presents polybutadiene) once the samples were quenched in cold water after blending.[58] However, no explanation had been given. We noticed that the used compatibilizer PS$_{100}$-*block*-PB$_{1111}$ was highly asymmetric and the longer PB block was extended into the minor PE phase. So, Fortelny's observations were actually consistent with the above discussion.

Co-continuous Intervals of the PS/PMMA System with the Fixed Dosage of the Asymmetric Polymeric Surfactants. For comparison, the PS/PMMA blends of the different PS/PMMA ratios without polymeric surfactants were prepared. A narrow cocontinuous interval from PS/PMMA = 45/55 to 50/50 was identified, as evident in Figure 4. Out of this composition window was the droplet-in-matrix structure.

Figure 5 shows the typical TEM images of the blends of different PS/PMMA ratios with 20% dosage of AB3 block copolymer. These TEM images revealed the cocontinuous interval of the PS/PMMA blend in the addition of the asymmetric polymeric surfactant. The cocontinuous interval of the PS/PMMA blends with 20% AB3, derived by the solvent extractions, is shown in Figure 6 and compared with the one of the PS/PMMA blend without AB3. In the PS/PMMA blends with 20% AB3, the cocontinuous interval in terms of PS homopolymer fraction in the homopolymers was moved and broadened to PS/PMMA = 20/80−30/70, compared with the cocontinuous interval of the PS/PMMA blends without AB3 at PS/PMMA = 45/55−50/50, as seen in Figure 6a. The width of the cocontinuous interval was doubled, from about 5% to 10% as the asymmetric block copolymer AB3 was introduced to the blend system. Also, the cocontinuous intervals in terms of the total PS fraction (PS homopolymer + PS block in the copolymer) in the blends (homopolymers + copolymer) are presented in Figure 6b. The cocontinuous interval of the PS/PMMA blends with AB3 was shifted to 32/68−40/60, which was still wider than that of PS/PMMA blends without the copolymer.

This phenomenon is different from the normal observations and understandings. Commonly, the addition of block copolymers and graft copolymers narrows the cocontinuous interval.[37,38] As discussed previously, the addition of the asymmetric copolymer might introduce the bending stress caused by the packing of the copolymer chains on the interface. This force should be against the breakup of the fibers of the dispersed phase when the longer block of the asymmetric block copolymer was located at the minor phase side of the interface as in the current case, favoring to form the cocontinuous morphology.

Comparison of PMMA-*b*-PS and P(S-*ran*-MMA)-*b*-PS Acting as the Polymeric Surfactants. Previously, we reported that the effect of the AC block copolymer of P(S-*ran*-MMA)$_{220}$-*b*-PS$_{320}$ on the morphology of the PS/PMMA blends.[59] The monomer composition in the random block of AC was set to be 0.5 to get the largest interfacial activity.[30] It was expected such rearrangement of the monomer units could reduce the effective χN between the two blocks and improve the solubility of the copolymers in the homopolymers (especially the PS phase). This

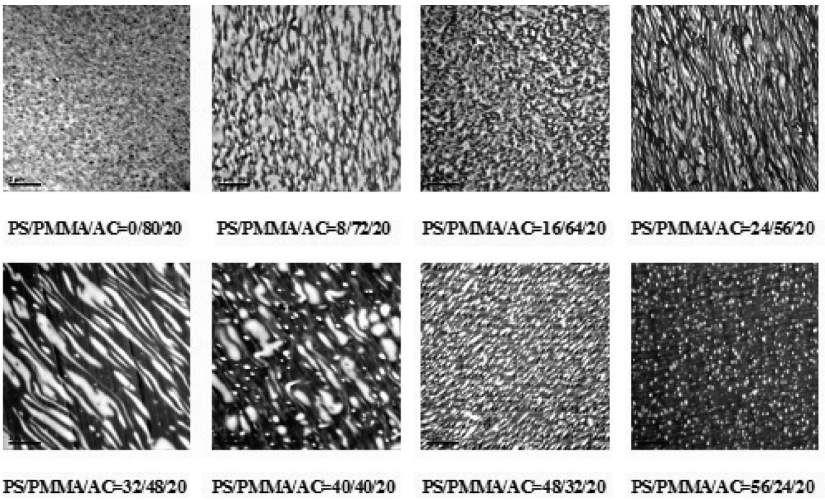

Figure 9. TEM images of the PS/PMMA blends of various composition with 20% asymmetric AC block copolymer, P(MMA-*ran*-S)$_{220}$-*b*-PS$_{320}$. The compositions of the blends are shown below each image. All the images are 11.5 μm × 11.5 μm.

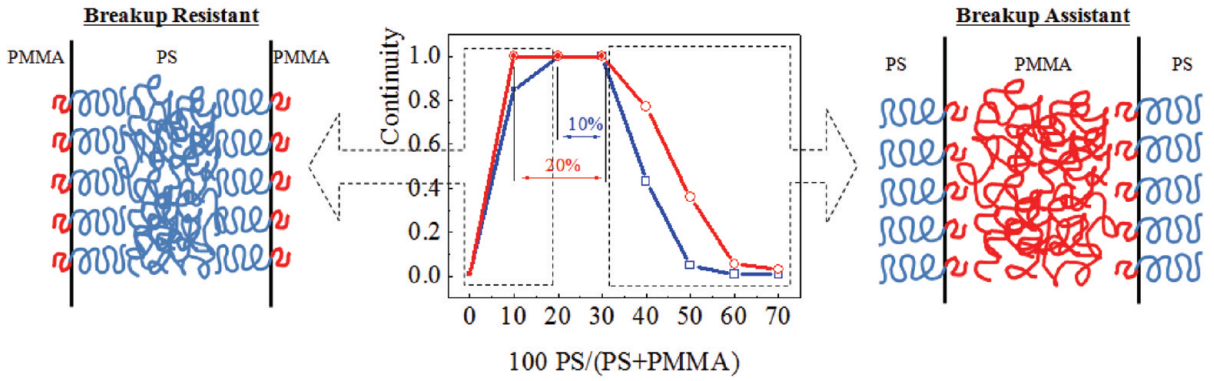

Figure 10. Cocontinuous interval of the PS/PMMA blends with 20% (red line + circle) P(MMA-*ran*-S)$_{220}$-*b*-PS$_{320}$, AC as surfactant, and with 20% (blue line + square) PMMA$_{110}$-*b*-PS$_{433}$, AB3 as surfactant. Continuity of PS (filled scatters) was detected by cyclohexane extraction and continuity of PMMA (hollowed scatters) was detected by formic acid extraction. The compositions of the blends should be expressed as PS/PMMA/copolymer = $0.8x/0.8(100 - x)/20$, where x is the PS homopolymer fraction in homopolymers.

AC block copolymer had the same molecular weight and monomer composition to the AB3 block copolymer in this current work.

The continuity curves of the PS phase versus the copolymer dosages were compared between the PS/PMMA = 30/70 blends with AC and with AB3, respectively. The PS phase continuity curves of the blends with AB3 and AC were almost identical as seen in Figure 7. The continuity of the PS phase increased as the dosage of the polymeric surfactant increased. At 20% of the copolymer dosage, the fully cocontinuous structure was achieved.

In Figure 8, it was clear that the AC block copolymer had much better emulsification effect than the AB3 block copolymer did for the PS/PMMA = 30/70 blends. At 20% dosage, AC reduced the characteristic size of the blend down to 100 nm, less than one-third of the AB3 did. One should notice that although there was a level-off after 5% dosage of AB3 and 10% dosage of AC, the new interface was still being generated because the continuity of the dispersed PS phase was still increasing. Since the interfacial activity of AB3 should be higher than AC,[30−32] such results revealed that the AC block copolymer should transport much faster than AB3 block copolymer from the PS phase to the interface.

Figure 9 shows the TEM images of the PS/PMMA blends with different PS/PMMA ratios but the fixed AC block copolymer dosage of 20%. The cocontinuous interval of the PS/PMMA blends added AC as polymeric surfactant is shown in Figure 10 and compared with the one of added 20% AB3. First, the positions of the cocontinuous intervals were almost the same for the blends with these two copolymers because the two copolymers had the same monomer compositions and molecular weights. Second, the cocontinuous interval of the PS/PMMA blends with 20% AC block copolymer was broadened to at least 20% in terms of PS homopolymer fraction in homopolymers, PS/PMMA = 10/90−30/70, which was even wider than the one in the case with 20% AB3 block copolymer, PS/PMMA = 20/80−30/70. The AC block copolymer could make the PS/PMMA = 10/90 blend form the fully cocontinuous structure.

The wider cocontinuous window in the presence of the AC block copolymer than the AB3 block copolymer may be due to that the AC block copolymer had higher asymmetry than the AB3 block copolymer although the compositions were the same. The both blocks of AB3 copolymer and PS block of AC were stretched in their corresponding homopolymer sides of the

dx.doi.org/10.1021/ma1026719 |*Macromolecules* 2011, 44, 2934–2943

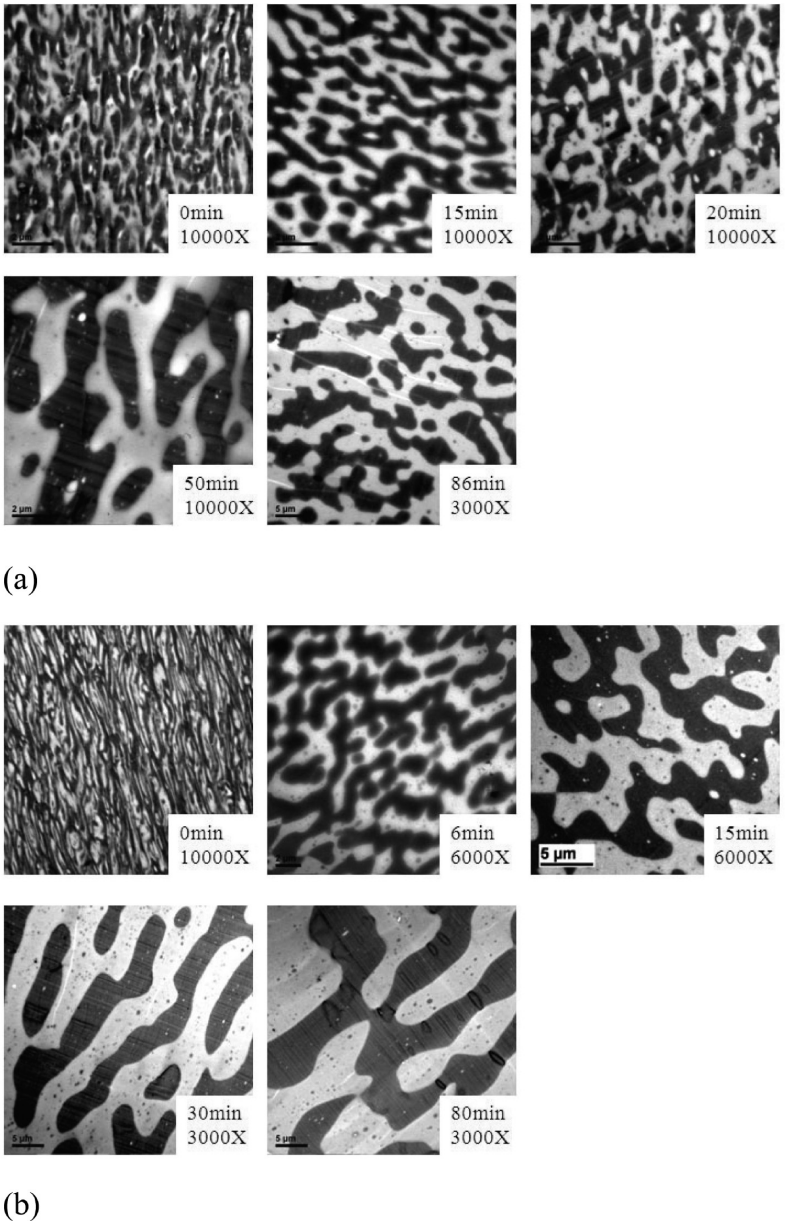

Figure 11. Thermal stabilities of the blends using AC and AB3 as polymeric surfactants respectively during annealing. The magnification ratios are listed below the annealing time in each image. (a) TEM images of annealed samples of the PMMA/PS/AB3 = 56/24/20 blends. (b) TEM images of the annealed samples of the PMMA/PS/AC = 56/24/20 blends.

interface,[60] while the random block of AC copolymer formed loops crossing the interface rather than stretched conformation in one side of the interface.[61,62] The asymmetry is actually the volume ratio of the two parts of a block copolymer chain respectively located in the minor phase side and in the major phase side of the interface. In the case of AC block copolymer, the looped random block would equally distribute on both sides of the interface since the molar composition was 0.5. Considering the fractional exponent relationship between degree of polymerization and the radius of gyration,[63] the asymmetry of AC should be much larger than that of AB3.

Such disparity of asymmetry between AC and AB3 did not appear in Figure 5 because in the PS/PMMA = 30/70 blend the asymmetry of AB3 was already large enough to tune the morphology of the blend to the cocontinuous structure. But when the homopolymer ratio approaching the lower limit of the cocontinuous interval (PS/PMMA = 10/90), the disparity of the asymmetries in AC and AB3 turned out.

Additionally, on the right side of the cocontinuous interval in Figure 10, the continuity of PMMA phase reduced slower in the case using AC block copolymer as surfactants compared with the one in the case using AB3 block copolymer. There, the phase inversion was taking place; i.e., the PS blocks of the copolymers became to be extended to the continuous phase and to control the coalescence process. In such cases, the asymmetry of copolymers should favor the droplet-in-matrix structure rather than the cocontinuous one since the bending energy and the interfacial energy would have the same curvature preference. However, the PS blocks in AC block copolymer was shorter than that in AB3 block copolymer so that the coalescence was more

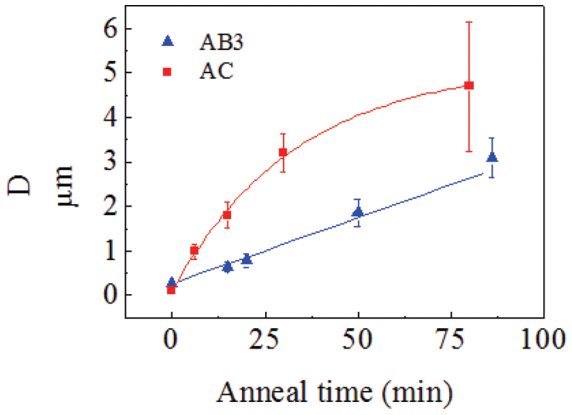

Figure 12. Characteristic size of the annealed samples of the blends: (blue line + triangle) PS/PMMA/$PMMA_{110}$-*b*-PS_{433}(AB3) = 24/56/20 (red line + square) PS/PMMA/P(S-*r*-MMA)$_{220}$-*b*-PS_{320}(AC) = 24/56/20.

likely to occur in the case with AC than in the case with AB3. According to the coalescence theory by Favis et al.,[10] after the cocontinuous interval, the structures reduced to droplet-in-matrix faster in the case with the AB3 block copolymer than in the case with the AC block copolymer.

The thermal stabilities of the cocontinuous morphology of the PS/PMMA = 30/70 blends with 20% AC and 20% AB3 block copolymers as polymeric surfactants are compared in Figures 11 and 12. The samples were annealed under vacuum at 200 °C for a certain time. First of all, the structure of the blends was not changed as evidenced in the TEM images during the annealing, although coarsening was obvious. Also, the results showed that the blend with AB3 block copolymer had better interfacial stability during annealing than the blend with AC block copolymer did. Torkelson et al.[64] reported that in the PS/PMMA/PS-*co*-PMMA blends the blend compatibilized by the gradient copolymer showed the best thermal stability during annealing among the blends compatibilized by the random copolymer and the block copolymer. Moreover, in the same work, they reported that the blend compatibilized by the random copolymer showed weaker stability than the blend compatibilized by the block copolymer.

The morphology evolution of the cocontinuous blends during annealing was clearly explained by Willemse,[65] Veenstra,[66] and Favis.[67] The driving force of coarsening during annealing is the capillary pressure from the size distribution of the minor phase domains. This pressure is proportional to the interfacial tension and inversely proportional to the rod thickness,[68] so that the thinner part of the cocontinuous structures undergoes larger capillary pressure and immerges into the thicker part spontaneously during the annealing. Because the blend with AB3 block copolymer as the surfactant should have lower interfacial tension than the blend with AC block copolymer as the surfactant, the blend using AC copolymer as surfactant showed weaker thermal stability than that using AB3 copolymer did.

In industry practice, reactive extrusion is often used to prepare the polymer blends. According to the above findings, well-designed lengths and branching structure of the reactive species to form the asymmetric copolymers in situ on the interface could promote the formation of the cocontinuous structure during reactive extrusion. Also, the reaction should be reactive enough to make sure the formation of a quite dense copolymer layer before the breakup of the stretched fibers.

4. CONCLUSION

We systematically investigated the influence of the asymmetry of the diblock copolymers being the polymeric surfactants on the morphology of the immiscible binary polymer blends of PS and PMMA. The following unexpected results were observed:

(1) With increase of the asymmetry of the AB diblock copolymer, the polymeric surfactant for the PS/PMMA blends, the cocontinuous morphology became more favored, as indicated by the broadened cocontinuous interval of the PS/PMMA system.

(2) AC block copolymer could provide higher asymmetry than the AB block copolymer at the same molecular weight and monomer composition. At 20 wt % AC dosage, the cocontinuous intervals of the PS/PMMA system spanned from PS/PMMA = 10/90 to 30/70.

It was believed that when the longer block of the asymmetric block copolymer packed on the minor phase side of the interface between the two homopolymers, the bending stress of the surfactant molecule layer could be against the interfacial tension to suppress the breakup of the minor phase fibers during melt mixing, which promoted the formation of the cocontinuous morphology.

For the first time, we demonstrated that the asymmetry of the diblock copolymer had significant influence on the morphology of the polymer blends in the melt mixing process. The asymmetry of the diblock copolymer could be a new parameter to tune the morphology.

AUTHOR INFORMATION

Corresponding Author

*E-mail: yingwu.luo@zju.edu.cn.

ACKNOWLEDGMENT

This work was financially supported by NSF of China under Grant 20774087 and Program for Changjiang Scholars and Innovative Research Team in University.

REFERENCES

(1) Veenstra, H.; Verkooijen, P. C. J.; van Lent, B. J. J.; van Dam, J.; de Boer, A. P.; Nijhof, A. *Polymer* **2000**, *41* (5), 1817–1826.

(2) Jouenne, S.; Gonzalez-Leon, J. A.; Ruzette, A.-V.; Lodefier, P.; Leibler, L. *Macromolecules* **2008**, *41*, 9823–9830.

(3) Potschke, P.; Bhattacharyya, A. R.; Janke, A. *Polymer* **2003**, *44* (26), 8061–8069.

(4) Frost, J. M.; Cheynis, F.; Tuladhar, S. M.; Nelson, J. *Nano Lett.* **2006**, *6* (8), 1674–1681.

(5) Salehi, P.; Sarazin, P.; Favis, B. D. *Biomacromolecules* **2008**, *9* (4), 1131–1138.

(6) Roy, X.; Sarazin, P.; Favis, B. D. *Adv. Mater.* **2006**, *18* (8), 1015–1019.

(7) Bates, F. S.; Maurer, W. W.; Lipic, P. M.; Hillmyer, M. A.; Almdal, K.; Mortensen, K.; Fredrickson, G. H.; Lodge, T. P. *Phys. Rev. Lett.* **1997**, *79* (5), 849–852.

(8) Fredrickson, G. H.; Bates, F. S. *J. Polym. Sci., Part B: Polym. Phys.* **1997**, *35* (17), 2775–2786.

(9) Rosedale, J. H.; Bates, F. S.; Almdal, K.; Mortensen, K.; Wignall, G. D. *Macromolecules* **1995**, *28* (5), 1429–1443.

(10) Li, J. M.; Ma, P. L.; Favis, B. D. *Macromolecules* **2002**, *35* (6), 2005–2016.

(11) Leclair, A.; Favis, B. D. *Polymer* **1996**, *37* (21), 4723–4728.

(12) Paul, D. R.; Barlow, J. W. *J. Macromol. Sci., Rev. Macromol. Chem.* **1980**, *C18* (1), 109–168.
(13) Willemse, R. C.; de Boer, A. P.; van Dam, J.; Gotsis, A. D. *Polymer* **1999**, *40* (4), 827–834.
(14) Matsen, M. W.; Bates, F. S. *J. Polym. Sci., Part B: Polym. Phys.* **1997**, *35* (6), 945–952.
(15) Matsen, M. W.; Bates, F. S. *J. Chem. Phys.* **1997**, *106* (6), 2436–2448.
(16) Matsen, M. W.; Bates, F. S. *Macromolecules* **1996**, *29* (4), 1091–1098.
(17) Matsen, M. W.; Schick, M. *Phys. Rev. Lett.* **1994**, *72* (16), 2660–2663.
(18) Helfrich, W. *Z. Naturforsch.* **1973**, *28C*, 693–703.
(19) Leermakers, F. A. M.; Barneveld, P. A.; Sprakel, J.; Besseling, N. A. M. *Phys. Rev. Lett.* **2006**, *97* (066103), 1–4.
(20) Chang, K.; Morse, D. C. *Macromolecules* **2006**, *39*, 7397–7406.
(21) Lee, J. H.; Ruegg, M. L.; Balsara, N. P.; Zhu, Y. Q.; Gido, S. P.; Krishnamoorti, R.; Kim, M. H. *Macromolecules* **2003**, *36* (17), 6537–6548.
(22) Lee, J. H.; Balsara, N. P.; Krishnamoorti, R.; Jeon, H. S.; Hammouda, B. *Macromolecules* **2001**, *34* (19), 6557–6560.
(23) Holmberg, K.; Jonsson, B.; Kronberg, B.; Lindman, B. *Surfactants and Polymers in Aqueous Solution*; John Wiley & Sons, Ltd.: New York.
(24) Yin, Z.; Koulic, C.; Jeon, H. K.; Pagnoulle, C.; Macosko, C. W.; Jerome, R. *Macromolecules* **2002**, *35* (24), 8917–8919.
(25) Lyu, S.; Jones, T. D.; Bates, F. S.; Macosko, C. W. *Macromolecules* **2002**, *35* (20), 7845–7855.
(26) Adedeji, A.; Lyu, S.; Macosko, C. W. *Macromolecules* **2001**, *34* (25), 8663–8668.
(27) Macosko, C. W. *Macromol. Symp.* **2000**, *149*, 171–184.
(28) Macosko, C. W.; Guegan, P.; Khandpur, A. K.; Nakayama, A.; Marechal, P.; Inoue, T. *Macromolecules* **1996**, *29* (17), 5590–5598.
(29) Sundararaj, U.; Macosko, C. W. *Macromolecules* **1995**, *28* (8), 2647–2657.
(30) Lyatskaya, Y.; Gersappe, D.; Gross, N. A.; Balazs, A. C. *J. Phys. Chem.* **1996**, *100* (5), 1449–1458.
(31) Lefebvre, M. D.; Dettmer, C. M.; McSwain, R. L.; Xu, C.; Davila, J. R.; Composto, R. J.; Nguyen, S. T.; Shull, K. R. *Macromolecules* **2005**, *38* (25), 10494–10502.
(32) Shull, K. R. *Macromolecules* **2002**, *35* (22), 8631–8639.
(33) Galloway, J. A.; Jeon, H. K.; Bell, J. R.; Macosko, C. W. *Polymer* **2005**, *46* (1), 183–191.
(34) Hu, Y. T.; Pine, D. J.; Leal, L. G. *Phys. Fluids* **2000**, *12* (3), 484–489.
(35) Milliken, W. J.; Leal, L. G. *J. Colloid Interface Sci.* **1994**, *166* (2), 275–285.
(36) Stone, H. A.; Leal, L. G. *J. Fluid Mech.* **1990**, *220*, 161–186.
(37) Willis, J. M.; Caldas, V.; Favis, B. D. *J. Mater. Sci.* **1991**, *26* (17), 4742–4750.
(38) Zhang, C. L.; Feng, L. F.; Zhao, J.; Huang, H.; Hoppe, S.; Hu, G. H. *Polymer* **2008**, *49* (16), 3462–3469.
(39) Luo, Y. W.; Liu, X. Z. *J. Polym. Sci., Part A: Polym. Chem.* **2004**, *42* (24), 6248–6258.
(40) Wang, R.; Luo, Y. W.; Li, B. G.; Sun, X. Y.; Zhu, S. P. *Macromol. Theory Simul.* **2006**, *15* (4), 356–368.
(41) Sun, X. Y.; Luo, Y. W.; Wang, R.; Li, B. G.; Liu, B.; Zhu, S. P. *Macromolecules* **2007**, *40* (4), 849–859.
(42) Galloway, J. A.; Koester, K. J.; Paasch, B. J.; Macosko, C. W. *Polymer* **2004**, *45* (2), 423–428.
(43) Li, J.; Favis, B. D. *Polymer* **2001**, *42* (11), 5047–5053.
(44) Lyu, S. P.; Bates, F. S.; Macosko, C. W. *AIChE J.* **2000**, *46* (2), 229–238.
(45) Lyu, S. P.; Bates, F. S.; Macosko, C. W. *AIChE J.* **2002**, *48* (1), 7–14.
(46) Cigana, P.; Favis, B. D.; Jerome, R. *J. Polym. Sci., Part B: Polym. Phys.* **1996**, *34* (9), 1691–1700.
(47) Broseta, D.; Fredrickson, G. H.; Helfand, E.; Leibler, L. *Macromolecules* **1990**, *23* (1), 132–139.
(48) Carton, J. P.; Leibler, L. *J. Phys. (Paris)* **1990**, *51* (16), 1683–1691.
(49) Chang, K.; Macosko, C. W.; Morse, D. C. *Macromolecules* **2007**, *40* (10), 3819–3830.
(50) Dai, K. H.; Kramer, E. J.; Shull, K. R. *Macromolecules* **1992**, *25* (1), 220–225.
(51) Bhadane, P. A.; Champagne, M. F.; Huneault, M. A.; Tofan, F.; Favis, B. D. *Polymer* **2006**, *47* (8), 2760–2771.
(52) Bourry, D.; Favis, B. D. *J. Polym. Sci., Part B: Polym. Phys.* **1998**, *36* (11), 1889–1899.
(53) Mekhilef, N.; Favis, B. D.; Carreau, P. J. *J. Polym. Sci., Part B: Polym. Phys.* **1997**, *35* (2), 293–308.
(54) Lyngaae-Jørgensen, J.; Rasmussen, K. L.; Chtcherbakova, E. A.; Utracki, L. A. *Polym. Eng. Sci.* **1999**, *39* (6), 1060–1071.
(55) Taylor, G. I. *Proc. R. Soc. London, Ser. A* **1932**, *138* (834), 41–48.
(56) Lepers, J. C.; Favis, B. D.; Tabar, R. J. *J. Polym. Sci., Part B: Polym. Phys.* **1997**, *35* (14), 2271–2280.
(57) Tomotika, S. *Proc. R. Soc. London, Ser. A* **1936**, *153* (A879), 0302–0318.
(58) Fortelny, I.; Hlavata, D.; Mikesova, J.; Michalkova, D.; Potrokova, L.; Sloufova, I. *J. Polym. Sci., Part B: Polym. Phys.* **2003**, *41* (6), 609–622.
(59) Pu, G. W.; Luo, Y. W.; Lou, Q. C.; Li, B. G. *Macromol. Rapid Commun.* **2009**, *30* (2), 133–137.
(60) Thompson, R. B.; Matsen, M. W. *J. Chem. Phys.* **2000**, *112* 6863–6872.
(61) Dai, C.-A.; Dair, B. J.; Dai, K. H.; Ober, C. K.; Kramer, E. J. *Phys. Rev. Lett.* **1994**, *73*, 2472–2475.
(62) James, E. W.; Soteros, C. E.; Whittington, S. G. *J. Phys. A: Math. Gen.* **2003**, *36*, 11575–11584.
(63) Rubinstein, M.; Colby, R. H. *Polymer Physics*; Oxford Univeristy Press: New York, 2003.
(64) Kim, J.; Gray, M. K.; Zhou, H. Y.; Nguyen, S. T.; Torkelson, J. M. *Macromolecules* **2005**, *38* (4), 1037–1040.
(65) Willemse, R. C.; Ramaker, E. J. J.; Dam, J. V.; Boer, A. P. D. *Polym. Eng. Sci.* **1999**, *39*, 1717–1725.
(66) Veenstra, H. B.; Lent, J. J. V.; Dam, J. V.; Boer, A. P. D. *Polymer* **1999**, *40*, 6661–6672.
(67) Yuan, Z. H.; Favis, B. D. *AIChE J.* **2005**, *51* (1), 271–280.
(68) Siggia, E. D. *Phys. Rev. A* **1979**, *20*, 595–605.